AAAI 1994 Spring Symposium on Medical Applications of Computer Vision

Shape-Based Grayscale Interslice Image Interpolation

William Barrett and Eric Bess

Department of Computer Science, Brigham Young University
Provo, UT 84602, barrett@cs.byu.edu

Abstract

A new algorithm for interpolation between grayscale serial slice images, such as from CT, is presented. The algorithm extends shape-based (SB) binary image interpolation to shape-based interpolation of grayscale images (SBIG). Unlike algorithms, such as linear (L) or cubic spline (CS) interpolation, which rely only on pixel position, SBIG makes essential use of object distance and morphology to interpolate between pixels and structures of similar shape and intensity which may differ in size and position from slice to slice. For reasonably low noise MRI, CT, and Cine CT grayscale images, results are superior visually and quantitatively (15%) to interpolation based solely on (x,y) proximity, particularly as the interslice spacing is increased. More importantly, while both L and CS interpolation demonstrate characteristic low-pass smearing of object edges and detail, these features are preserved and well approximated with SBIG. As a result, reconstructed coronal and sagittal slices from a densely interpolated image volume using SBIG demonstrate significantly clearer representation of anatomical structures and less "staircasing" than those created using either L or CS interpolation. Clipping artifacts due to nonoverlapping structures or rapid changes in image brightness are minimized using simulated three-dimensional distance maps.

Introduction

Acquisition of serial cross-sectional slice images has become ubiquitous in medical imaging. Because interslice spacing is typically greater than intraslice spacing, image interpolation techniques often are used to fill in the interslice spaces and produce a uniformly dense image volume.

A variety of linear, trilinear, and spline-based image interpolation techniques[1-3] have been used to fill the interslice spaces. However, the fundamental problem with each of these techniques is that an interpolated value $I'(x,y)$ is based only on image intensities at or near the same (x,y) position in the original adjoining slices I_j and I_{j+1} (Fig. 1). Thus, if the cross-sectional morphology of individual structures changes or is displaced significantly from slice to slice, image intensities from one tissue type may be averaged with those of another (Fig. 1a), causing spurious interpolated tissue intensities $I'(x,y)$ and an overall blurring throughout the interpolated image I'. Hence, image interpolation based on (x,y) position alone often does not provide an appropriate correspondence between structures of the same tissue type in adjoining slices, especially near object boundaries. This problem is accentuated as the interslice spacing increases.

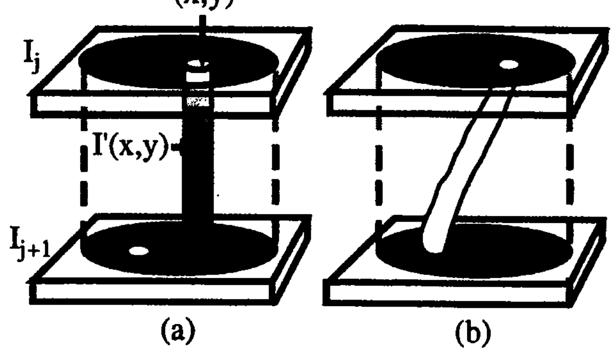

Figure 1. (a) Interpolation which averages between different tissue types. (b) ideal interpolation.

Shape-based Binary Interpolation

Shape-based interpolation (SB) greatly reduces the dependency on (x,y) position, but has been applied successfully only to binary (segmented) images[4], with some improvement resulting from superior estimation of euclidean distance[5]. SB has also been combined with grayscale interpolation to produce more accurate binary interpolations[6-7]. However, SB has only recently been applied directly to the interpolation of grayscale images[8].

SB requires that a distance map, D, be computed for each slice. The convention here is to use positive values for pixels interior to an object and negative values for pixels exterior to the object. For example, let B_j and B_{j+1} represent corresponding rows from two adjacent binary image slices (Fig. 2). Let D_j and D_{j+1} represent the dist-

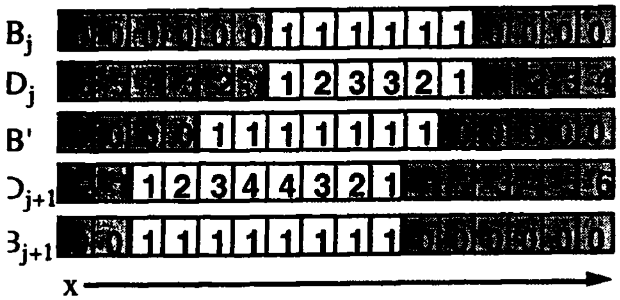

Figure 2. Shape-based binary interpolation.

ınce maps for B_j and B_{j+1}. The interpolated biıary slice, B', is obtained by thresholding (≥0) he weighted average of D_j and D_{j+1}. For :xample, $B'(x=6) = 1$ since $.5[D_j(6)+D_{j+1}(6)] = 5[-1 + 4] = 1.5 \geq 0$, assuming B' is midway (.5) ıetween B_j and B_{j+1}.

;hape-based Grayscale Interpolation

The SB algorithm is applied to interpolation of ;rayscale images by treating them as n binary mages, $B_k(x,y)$, k =1...n where n is the bit-depth esolution of the original grayscale images I_j and $_{j+1}$. Specifically, the interpolated image

$$I'(x,y) = \max [B'_k(x,y)], \text{ for } k = 1 \text{ to } n. \quad [1]$$

'or example, if I_j is an 8-bit image, then n = 255. f each B_k is defined by a thresholding operation n the original image, such that

$$B_k(x,y) = k \text{ for } I_j(x,y) \geq k \quad [2]$$
$$= 0, \text{ otherwise}$$

ıen I_j can be exactly represented as

$$I_j(x,y) = \max_k [B_{k,j}(x,y)]. \quad [3]$$

'hus, an interpolated grayscale image slice, I', etween two adjoining images I_j and I_{j+1} can be btained by first applying equation [2] to I_j and $_{+1}$ separately to produce corresponding binary nages $B_{k,j}$ and $B_{k,j+1}$, for each k =1...n, and then pplying the SB binary algorithm to obtain an ıterpolated binary image B'_k, for each $(B_{k,j}, _{k,j+1})$, k =1...n.

$$B'_k = SB\ (B_{k,j}, B_{k,j+1}) \quad [4]$$

he final interpolated grayscale image, I', is then obtained by maximizing over all B'_k, as shown in equation [1].

One of the problems with SBIG is that if an object is present in one of the original slices, but absent in the next, the object may be clipped abruptly. However, this can be partially overcome by combining 2D distance maps from the original slices, I_j and I_{j+1}, with a simulated 3D distance map in order to linearly extrapolate the clipped structure from one slice to the next (SBIG+).

Results

The complexity of the SBIG algorithm is O(Ng) time and O(Ng) memory, where N = number of pixels in the image and g = number of gray levels. The SBIG algorithm has been implemented on an HP 700 workstation. Compute times for a $256^2 \times 8$ image are 2.1, 4.3, and 430 seconds for L, CS, and SBIG respectively.

Visual Comparison

Comparison of SBIG with linear (L) and cubic spline (CS) interpolation, is performed by excluding an image slice, I_j, from a set of serial slices and then attempting to recreate I_j by interpolating between I_j's neighboring slices, I_{j-1} and I_{j+1}. Let I_L, I_C, and I_S represent I_j recreated using L, CS, and SBIG, respectively. This type of comparison is first applied to two of eight 8mm thick Cine CT scans through the opacified left ventricle at end diastole. Figures 3a-c show the original third ($I_{j-1}=I_3$), fourth ($I_j=I_4$), and fifth ($I_{j+1}=I_5$) slices. Slices I_3 and I_5 are separated by a 12mm gap. The objective is to recreate I_4 by interpolation. I_4 is recreated in figures 3d-f by applying L, CS, and SBIG interpolation respectively to slices I_3 and I_5.

Note that the SBIG algorithm *preserves* high frequency image features such as left ventricular, myocardial, and lung boundaries. Also, the structure of the left ventricle is reasonably well approximated by SBIG, whereas L and CS interpolation *introduce* low frequency information and intermediate pixel intensities (not present in I_3 and I_5) by averaging pixel intensities from differing tissue types. This is particularly noticeable along the myocardial-lung and left ventricular-myocardial boundaries.

SBIG was applied to the entire cardiac Cine CT image set, resulting in 103 total (8 original + 95 interpolated) slices from which reconstructed coronal slices were extracted (Figure 4a). The same reconstructed coronal slice obtained from L and CS are shown in figures 4b and 4c. The smearing effect found in the L and CS cross-sectional slices is even more pronounced in the coronal view, while the coronal view produced by SBIG demonstrates well-defined anatomical boundaries and overall smoother representation of object structure.

Sagittal views were also reconstructed from a CT data set of the head containing 64 original abutting scans, 1.5mm thick. Comparisons were performed using only 15 of the original 64 slices. A mid-sagittal view comprised of all 64 slices (linearly interpolated = gold standard) is shown in figure 5a. Corresponding sagittal views for SBIG L, and CS, (shown in figures 5b-d) consist of a total of 226 (210 interpolated) slices. Note that the smearing artifacts associated with L and CS are still present, while object boundaries such as skull and skin are more faithfully represented with SBIG. SBIG also avoids "ghosts" (i.e. artificial intermediate pixel intensities which occur in L or CS (Fig. 6). However, figure 5b does demonstrate some of the limitations of SBIG. Namely, if objects fail to overlap from slice to slice, pixel intensities produced by SBIG will diminish, as demonstrated by the soft vertical banding in the skull. Also, if an object is present in one of the original slices, but absent in the next, the object may be clipped abruptly. This can be seen when comparing Fig. 5b with 5a and 7b with 7a where clipping is perceived as a diminished intensity in the bony anatomy. However, this is overcome using a simulated 3D distance map (SBIG+, Fig. 7c).

Quantitative Comparison

Quantitative comparison of L, CS, and SBIG is obtained by computing error measures $E_L=|I_j-I_L|$, E_C $|I_j-I_C|$ and $E_S=|I_j-I_S|$ as a function of the number of slices skipped. The average error for E_S is consistently lower than that for E_L and E_C by about three gray levels per pixel, or about 15% less overall. In general, except for very closely spaced I_{j-1} and I_{j+1}, results show $E_S < E_L$, E_C, especially as the distance between I_{j-1} and I_{j+1} increases.

Conclusion

SBIG has been applied successfully to CT, Cine CT, and MRI grayscale images. For reasonably low noise images, results are superior visually and quantitatively to interpolation based solely on (x,y) proximity. This is particularly true as the interslice spacing increases. Of greatest significance is the omission of low frequency blurring and artificial intensities associated with L and CS and the preservation of sharp, distinguishable anatomical structures and boundaries. SBIG is more of a content based interpolation technique than L or CS in that it attempts to preserve similar regions from the original data slices that have changed in size, position or shape. SBIG is usually fairly successful in handling these changes, especially for larger regions and where the regions overlap. It is less successful at preserving small, rapidly changing regions. A summary of features and liabilities follows.

Features of SBIG:

- Does not introduce artificial image intensities
- Omission of low frequency blurring
- Preservation of sharp anatomical boundaries.
- Visual and quantitative improvement for low noise images.
- Possibility of requiring fewer original slices.

Liabilities:

- Computationally more expensive.
- Contouring and "patchy" appearance in noisy areas.
- Loss of structure in nonoverlapping regions.
- Object clipping if the object only appears in one original slice

References

1. S. Raya, J. Udupa, and W. Barrett: "A PC-Based 3D Imaging System: Algorithms, Soft-ware, and Hardware Considerations." *J. of Comp. Med. Imaging and Graphics*, Vol. 14, Number 5, :353-370, March, 1990.
2. C. Upson and M. Keeler, "V-Buffer: Visible Volume Rendering," *Computer Graphics* 22 (4) :59-64, 1988.
3. R. Burden and J. Faires, *Numerical Analysis*. Prindle, Weber & Schmidt, Boston MA, 1985.
4. S. Raya and J. Udupa, "Shape-based Interpolation of Multidimensional Objects," *IEEE Trans. on Medical Imaging*, 9(1) :32-42, 1990.
5. G. Herman, "Shape-based Interpolation," *Computer Graphics and Applications*, Vol. 12, (3) :69-79, 1992.
6. R. Lotufo, G. Herman, and J. Udupa, "Combining Shape-based and Gray-level Interpolations," *Vis. Biomed Comput.* SPIE Vol. 1808, :289-298, 1992.
7. W. Higgins, et al., "Shape-Based Interpolation of Tree-Like Structures in Three-Dimensional Images," IEEE Trans Med Imag, V. 12, No. 3, :439-450, Sept. 1993.
8. R. Stringham and W. Barrett, "Shape-Based Interpolation of Grayscale Serial Slice Images," SPIE Medical Imaging: Vol. 1898 Image Processing, :105-115, 1993.

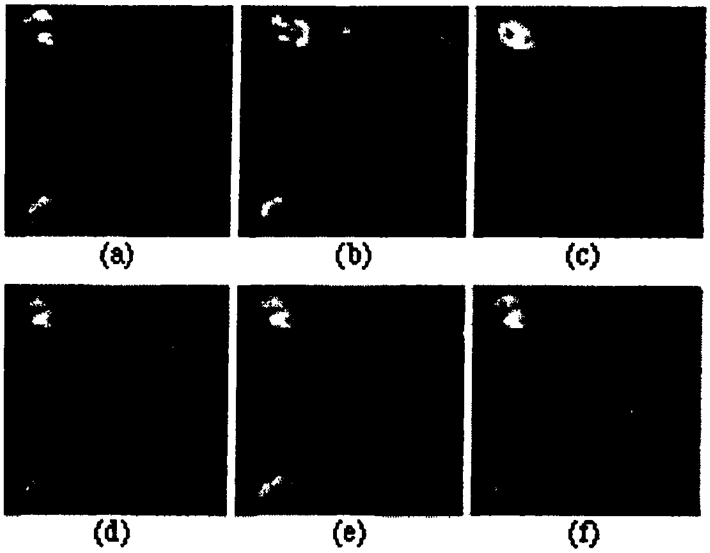

Fig. 3 (a-c) Original slices 3, 4, and 5 through the left ventricle. (d-f) Reconstruction of slice 4 (b) using (d) linear interpolation (e) cubic spline interpolation and (f) SBIG.

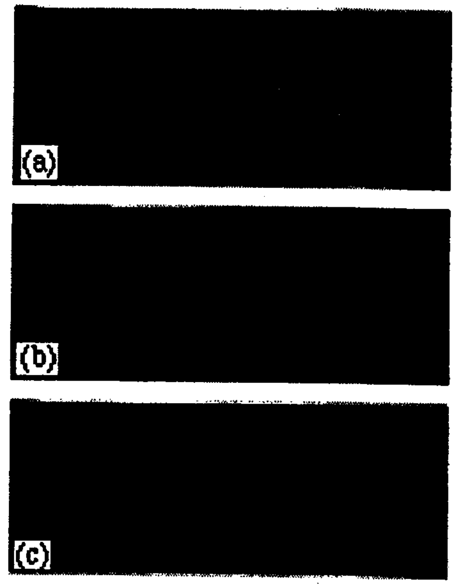

Fig. 4 Coronal view (103 slices, 8 original) using (a) SBIG (b) linear (c) cubic spline.

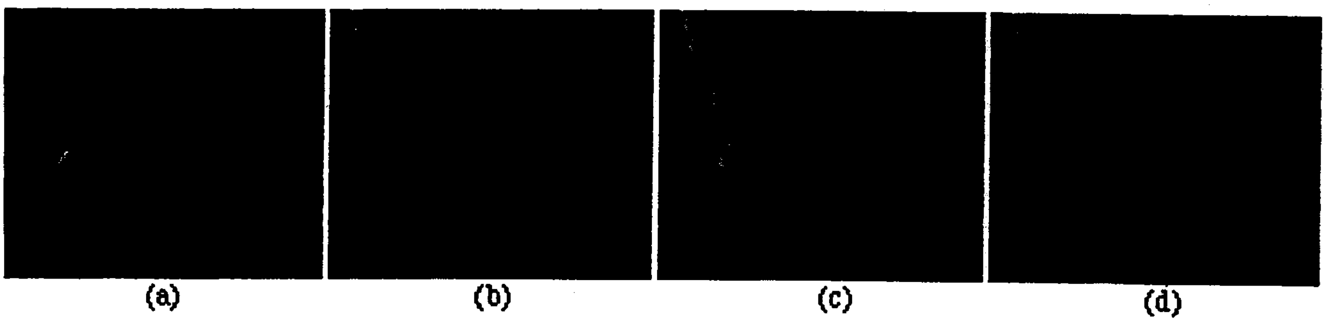

Fig. 5 Mid-sagittal reconstruction using (a) 64 original slices, 162 linearly interpolated, 226 total. (b-d) 15 of 64 original slices, 211 interpolated, 226 total using (b) SBIG (c) linear (d) cubic spline.

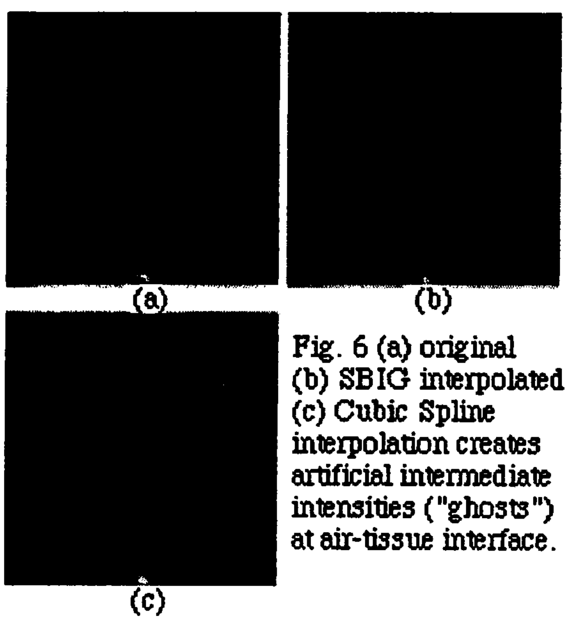

Fig. 6 (a) original (b) SBIG interpolated (c) Cubic Spline interpolation creates artificial intermediate intensities ("ghosts") at air-tissue interface.

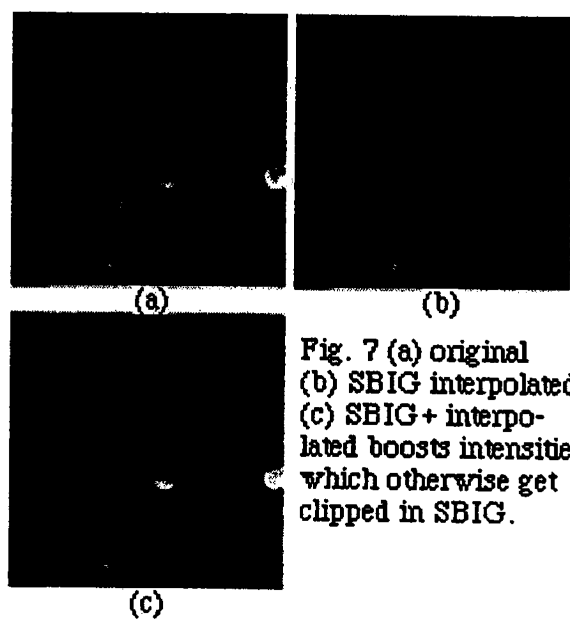

Fig. 7 (a) original (b) SBIG interpolated (c) SBIG+ interpolated boosts intensities which otherwise get clipped in SBIG.